Using a wearable micro-camera for dynamic glare evaluation: corrections and verification assessment

Abel Sepúlveda[1*], Caroline Karmann[1,2], and Jan Wienold[2]

[1]Karlsruhe Institute of Technology (KIT), Karlsruhe, Germany
[2]École Polytechnique Fédérale de Lausanne (EPFL), Lausanne, Switzerland

Abstract. Micro-cameras such as the 'vision-in-package' (VIP) can be used as a wearable for user-centric glare estimations. Yet, there is a lack of methodologies to use such head-mounted device and their outputs to obtain reliable glare evaluations. This paper focuses proposes a methodology for dynamic glare evaluation based on wearable micro-cameras. The methodology involves a novel image rotation algorithm and pixel overflow correction based the solar disk luminance measured using an HDR camera. We tested the methodology during an experiment where 21 participants were exposed to direct sunlight in an office-like set-up in Lausanne, Switzerland. For our dataset, the pixel overflow correction avoids an underestimation of the DGP metric in 94.8% of the cases. These corrections appear crucial for the correct estimation of glare using wearable VIP cameras.

1 Introduction

People spend on average about 90% of their time indoors [1]. Although daylight has been proved key to improve human circadian rhythms [2,3] and mental performance [4], excess of daylight levels in indoor spaces could lead to visual discomfort due to daylight glare [5] leading to a reduce of the comfort, performance, and ultimately, health of the building occupants [6]. Daylight glare is a complex phenomenon that depends on many factors [7] and could be challenging and expensive to assess in practice by designers and scientists [8].

The capture of luminance maps of the building occupants' FOV is necessary to accurately capture glare when high luminance sources (e.g., the sun) are in the field of view (FOV) of the occupants. Luminance maps are the primary input of glare metrics [9]. Luminance maps are typically saved as High Dynamic Range (HDR) images, where each pixel has associated a luminance value (e.g. in cd/m^2). Thus, glare metrics can be calculated from HDR images by using available tools such as *evalglare* function from the well-known Radiance software [10]. However, HDR images are produced using a costly and large camera, which means that glare is assessed punctually from the observer's position and with the assumption that the person is looking straight ahead. So far this has made dynamic glare estimation very complex, requiring head- and eye-tracker, sometimes backed with simulation tools.

* Corresponding author: abel.luque@kit.edu

The emergence of new micro cameras opens up new opportunities for dynamic glare assessment motived by hypotheses from previous investigations such as the dynamic-gaze behaviour of building occupants avoid glare discomfort [11].

The HDR vision sensor (VIP) is a 6 cm^3 device that has been used to integrate real-time visual comfort assessment in building automation systems. It can directly generate a HDR image, from which an embedded image processing software similar to *evalglare* can compute the DGP metric [12,13]. Yet, VIP cameras can only capture a limited luminance range and therefore might not be reliable when the sun-disk is in occupants' field of view [14]. Further it was observed that participants tilt their head unconsciously towards the side. In reality, the Vestibulo-ocular Reflex (VOR) helps to maintain a stable image on the retina by generating compensatory eye movements that are usually equal in magnitude but opposite in direction of the head rotation [15]. The VIP camera does not compensate internally participants' head rotation. Thus, these "tilted" images do not represent the perceived environment of the participants.

1.1 Aim and novelty of this investigation

This paper proposes a methodology for dynamic glare evaluation based on wearable micro-cameras VIP. Specifically, the objectives of this investigation are:
- To develop a methodology to correct the HDR images taken by VIP wearable micro-cameras;
- To quantify the impact of the rotation and pixel replacement algorithms on the DGP output, hereby verifying the methodology.

The proposed methodology will be critical to include future studies, the dynamic position of head movements in glare quantification, thereby paving the way for a truly human-centric estimation of discomfort glare.

2 Methodology

The methodology is based on previous work on the VIP camera and focuses on its use in the case of glare estimation, which involves two steps: (1) image rotation completed by a novel algorithm using image processing techniques (2) pixel overflow correction completed by replacing the sun disk from the VIP image output with that of the high-quality LMK camera.

We tested this methodology in the framework of a lab study pertaining to discomfort glare for different window transmittance. The experiments took place at the EPFL Campus, Lausanne, Switzerland between 25th May 2023 until 29th July 2023. We exposed participants (n=21) to scenario where they had the sun in the field of view. Each exposure lasted 30' and participants were wearing the VIP camera on their forehead. In the framework of this paper, we are mainly interested in the image correction procedure and not in participant's subjective glare responses.

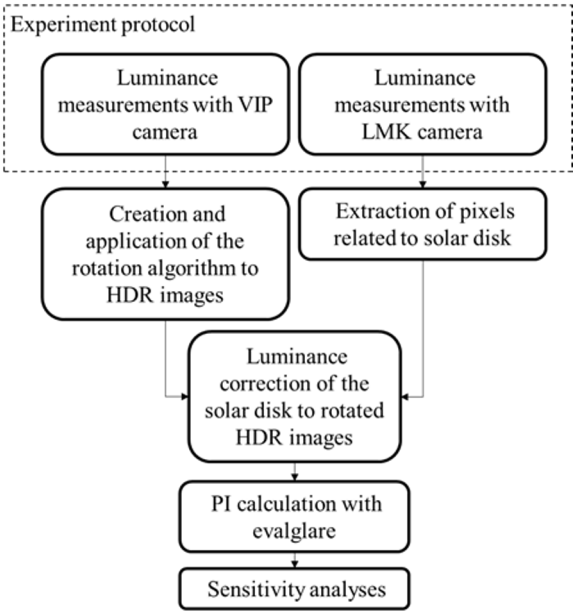

Fig. 1. Workflow followed in this investigation.

2.1 Image capture

Two types of luminance images where recorded: during the experiment, every 30 seconds, via the VIP camera and twice during the experiment (after 5' and 35' of exposure) via a high grade LMK camera.

(1) We continuously used VIP vision-in-package M12 camera (10-bit capture) with SD card and adapted 3D printed holder, with power input via microUSB or battery pack [16]. We used a 558BP100 Photopic Filter (12.5mm diameter, 2.3mm +/-0.2 thickness) ≥ 95% peak to occur within 553-557nm < 3% integrated error from CIE 1931 Photopic Luminosity Standard filter and SVL-01020B5M - 1.08MM S-Mount Fisheye Lens. The device was mounted on the forehead of participants with a GoPro headstrap and 3D printed plastic platform and anchor (Fig. 2). Each 30 seconds, this device recorded a 267x267 pixels format image.

In addition to the VIP images, we also punctually capture HDR images with the LMK camera to could extract the pixels related to the sun disk in order to replace the non-reliable sun pixels from HDR images obtained by the VIP camera.

2.2 Rotation algorithm

Since images generated by VIP camera were tilted according to each participant head movement had during the experiment (Fig. 2), we had to correct the rotation deviations (Fig. 3). We developed a detection-rotation algorithm in Python with well-known library image processing library cv2 [17]. There were not valid images because of high deviation in the field of view of the participant, presence of people in the field of view, and errors in the conversion to HDR format. Thus, we cleaned the VIP HDR images according to this criterion for each participant leading to the conclusion that between 71% and 95% (mean of 82%) of the converted HDR images were valid and therefore suitable to be rotated with the developed

algorithm. Thus, 81.7% of the generated HDR images were valid. The developed rotation algorithm consisted on 8 steps (Fig. 4):

Step 1 – Conversion of .hdr image from VIP measurements into grey scale image;

Step 2 – Application of Sobel transformation in X direction to grey scale image;

Step 3 – Selection of pixels with a value of 255 (white pixels);

Step 4 – Image cropping according to parameters lineCenter (height from bottom of the image where the cropped image has the centroid: 0.45) and margin (height of the new cropped image: 70 pixels);

Step 5 – Identification of pixel profile for each vertical profile;

Step 6 – Identification of the monitor screen frame pixels with filter based on maximum gradient (maxGrad=1.1);

Step 7 – Linear fitting of the monitor screen frame pixels (pixels located between 30% and 75% of the cropped image) and rotation angle calculation (α);

Step 8 – Rotation of the .hdr image using the Radiance command *pinterp* considering –α°.

Fig. 2. Micro HDR imager, aka. the "VIP" camera. This camera was equipped with a fish eye lens and a head strap to be used as a wearable [16].

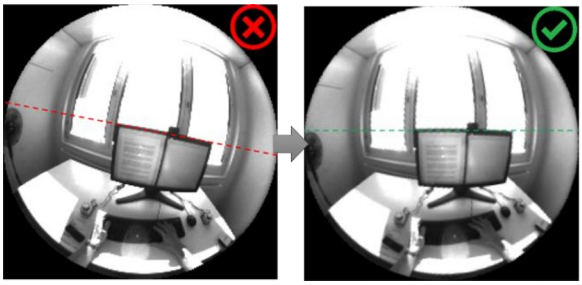

Fig. 3. HDR image from VIP camera output (left), and corrected HDR image after the rotation algorithm applied (right).

2.3 Pixel correction procedure

We computed discomfort due to glare using DGP, by running *evalglare* version 3.02 with default settings on the calibrated HDR images, which were analyzed for pixel overflow: images with measured vertical illuminance values were substantially higher (>25%) than the image-derived vertical illuminance values, were corrected by replacing the overflow pixels matching the measured vertical illuminance. In addition, the location of the sun position within each HDR image was identified as the brightest and largest glare source generated by *evalglare* (option -d). The pixel correction procedure must be applied to rotated HDR images in order to match Ev.

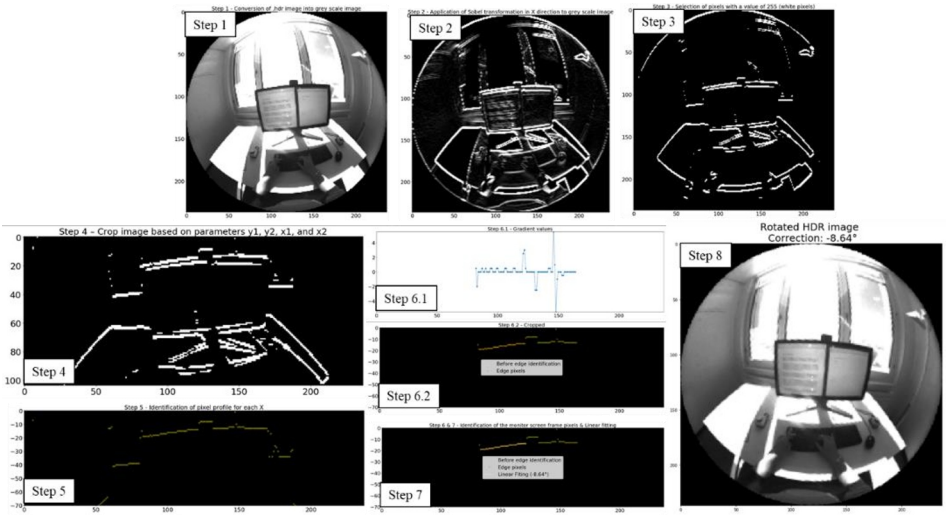

Fig. 4. Example of application of the developed detection-rotation algorithm step by step.

3 Results

3.1 Reliability of the rotation algorithm

The identification of wrong and well rotated images was made via visual inspection of the rotated HDR images by the algorithm. The percentage of successfully rotated HDR images with the detection-rotation algorithm (Fig. 4) was between 80.9% and 99.6% for any participant. The total accuracy of the developed algorithm was 93.4%. Therefore, we considered in average per participant 660 images to compute the dynamic glare assessment.

3.2 Position Index sensitivity with rotation correction

The first step of the proposed methodology pertains to the rotation of tilted images. At this stage of the analysis, the images are not yet corrected for pixel overflow.

In Fig. 5, we show the correlation in terms of Guth´s Position Index (P) between related to non and rotated HDR images. Given that the pixel overflow correction is the following step of this process, we found more relevant to quantify the impact of the rotation correction using the position index P. P depends on the location of the glare source and not on its luminance value. P ranges from 1 to 16. Given that P is used as squared value in the denominator in glare metrics, higher number lead to smaller glare estimates.

Minimum, median, maximum and standard deviation values can be seen in Table 1. The absence of correction for tilted HDR images can lead to an overestimation of P for 39.8% of the images and an underestimation 23.8% of the images (i.e., points respectively above and below the black dotted line in Fig. 5).

Table 1. Minimum (min), maximum (max), mean, median and standard deviation (SD) of Position Index values before (Pnu) and after rotation (Pru).

	min	**max**	**mean**	**median**	**SD**
Pru	1	16	9.36	8.59	4.36
Pnu	1	16	9.25	8.51	4.38

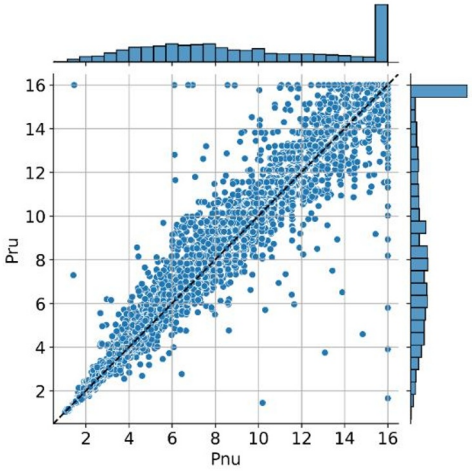

Fig. 5. Correlation between P obtained from rotated (Pru) and non-rotated (Pnu) of uncorrected HDR images.

3.3 DGP sensitivity with pixel overflow correction

The second step of the proposed methodology is to quantify the change in predicted discomfort glare following pixel-overflow correction.

In Fig. 6, we show the correlation in terms of DGP between pixel-corrected and pixel-non corrected images. At this stage, all images have been rotated. Minimum, median, maximum and standard deviation values can be seen in Table 2. The missing pixel overflow correction of rotated HDR images would lead to an underestimation of 94.8% of the DGP values (points above the dotted black line) and an overestimation of 4.7% of the DGP values (points below the dotted black line: 0.3% of the images).

The adequation between DGP from corrected and uncorrected images is higher for lower values (DGP<0.20) and higher values (DGP>0.5).

Table 2. Minimum (min), maximum (max), mean, median and standard deviation (SD) of Position Index values before (Pnu) and after rotation (Pru).

	min	**max**	**mean**	**median**	**SD**
DGPnc	0.16	1	0.419	0.409	0.089
DGPrc	0.16	1	0.418	0.407	0.089
DGPru	0.16	1	0.286	0.279	0.056

3.4 Glare discomfort sensitivity with proposed methodology

Lastly, we quantified the relative shift in discomfort glare classes (following DGP estimates) for each step. In Fig. 7 we are showing the output without any correction (aka., DGPnu, in blue), with rotation correction (aka., DGPru, in orange), without rotation but with pixel correction (aka., DGPnc, in yellow), and with both rotation and pixel-overflow correction (DPGrc, in grey). As can be seen on Fig. 7, for any glare discomfort category, the number of cases for DGPnu and DGPru are similar. The rotation algorithm does not have a significant impact on glare discomfort classes for the pixel-corrected HDR images: reduction of 0.17% of “intolerable” glare cases, reduction of 0.06% of “disturbing” glare cases, increase of 0.14% of “imperceptible” glare cases and increase of 0.09%) “noticeable” glare cases. This small

deviations in DGP are in line with the small differences in P shown in Table 1. A missing tilt correction of the images from VIP cameras does not lead to significant underestimation of glare.

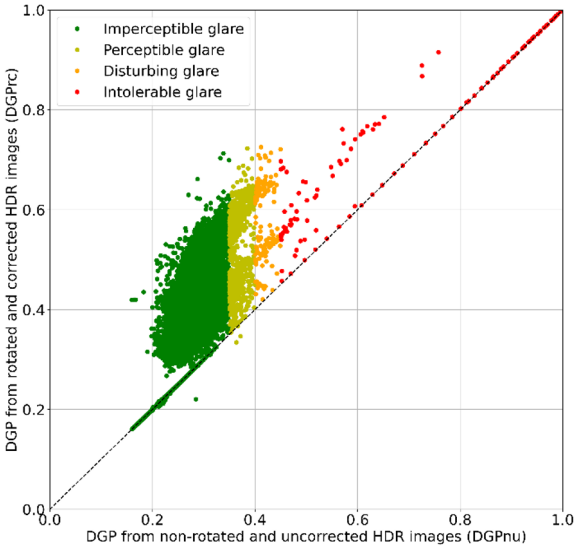

Fig. 6. Correlation per glare category between DGP obtained from corrected (DGPrc) and uncorrected (DGPru) of rotated HDR images.

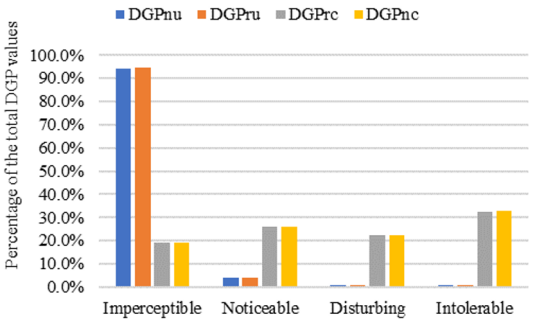

Fig. 7. Percentage of the DGP values falling in different glare discomfort categories in different stages of the applied methodology. n=non-rotated, r=rotated, c=corrected, and u=uncorrected.

4 Discussion

The reliance on a high-quality LMK camera to correct pixel overflow may present a drawback due to the necessity of merging two distinct systems, potentially causing obstacles in practical use and escalating both the intricacy and expenses of the setup. Furthermore, the mismatch in timing between the LMK and VIP cameras could introduce inaccuracies, given the assumption of consistent and unobstructed sky conditions are challenging to ensure during experiments. In order to reduce this mismatch, future experiments could have shorter time intervals between LMK and VIP measurements. In addition, to consider larger and more diverse participant group would be needed to validate the methodology across different user profiles. To enhance the proposed methodology, it could be advantageous to investigate methods or technological advancements that expand the luminance range directly within the

VIP camera without the need for external high-grade cameras as the LMK luminance camera. For instance, the addition of a ND filter can significantly expand its maximum usage range [14].

5 Conclusion

This paper focuses on the limitation of the VIP camera when exposed to large luminance sources (above 30 kcd/m^2) and proposes a methodology for dynamic glare evaluation using the VIP as a wearable micro-camera when the sun in one's field of view. This methodology involves a novel image rotation algorithm and a pixel overflow correction. We tested the methodology with data from an experiment involving 21 participants (14586 captured images) taking place in Lausanne, Switzerland between May and July 2021.

According to our results, the absence of correction for tilted HDR images does not lead to a significant misclassification (overestimation or underestimation) of discomfort glare categories. Nevertheless, the lack of pixel-correction can underestimate glare (from intolerable to the others glare categories) in 72% of the HDR images obtained with the VIP camera. We recommend the use of the proposed methodology when evaluating dynamic glare with VIP cameras since HDR images generated by these ones are not reliable enough for glare evaluation.

We would like to thank Edoardo Franzi for his support in setting up the VIP camera using dedicated computer scripts. We would like to thank Geraldine Quek and Dong Kim for their support in setting up, calibrating and characterizing the VIP camera.This study was funded by Swiss National Foundation project (SNF) grant for the project "Visual comfort without borders: interactions on discomfort glare" number 200020_182151.

References

1. *M. Awada, B. Becerik-Gerber, S. Hoque, Z. O'Neill, G. Pedrielli, J. Wen, and T. Wu, Build Environ **188**, (2021)*
2. *R. Samuels, Energy and the Environment. Into the 1990s. Proceedings of the 1st World Renewable Energy Congress|Energy and the Environment. Into the 1990s. Proceedings of the 1st World Renewable Energy Congress (1990)*
3. *H. Sanaieian, M. Tenpierik, K. Van Den Linden, F. M. Seraj, and S. M. M. Shemrani, Renewable and Sustainable Energy Reviews (2014)*
4. *M. B. C. Aries, J. A. Veitch, and G. R. Newsham, J Environ Psychol **30**, (2010)*
5. *C. Pierson, B. Piderit, T. Iwata, M. Bodart, and J. Wienold, Lighting Research and Technology **54**, (2022)*
6. *M. B. C. Aries, J. A. Veitch, and G. R. Newsham, J Environ Psychol **30**, (2010)*
7. *W. K. E. Osterhaus, in Solar Energy (2005)*
8. *A. Sepúlveda, B. Bueno, T. Wang, and H. R. Wilson, Build Environ **201**, 15 (2021)*
9. *J. Wienold and J. Christoffersen, Energy Build (2006)*
10. *J. Wienold, Evalglare – A New RADIANCE-Based Tool to Evaluate Daylight Glare in Office Spaces (3rd International RADIANCE Workshop, 2004)*
11. *M. Sarey Khanie, (2015)*
12. *A. Motamed, L. Deschamps, and J. L. Scartezzini, Energy Build **203**, (2019)*
13. *A. Motamed, B. Bueno, L. Deschamps, T. E. Kuhn, and J. L. Scartezzini, Build Environ **171**, (2020)*

14. *D. H. Kim, G. C. T. Quek, and J. Wienold, in (International Commission on Illumination, 2023), p. 10*
15. *A. M. and L. R. Wellings Thomas P. and Brichta, in Encyclopedia of Computational Neuroscience, edited by R. Jaeger Dieter and Jung (Springer New York, New York, NY, 2013), pp. 1–4*
16. *CSEM, (n.d.)*
17. *OpenCV Team, 2023 (n.d.)*